Low-Temperature Plasma Physics

Lecture Script

November 2026

Preface

This script follows the eight-part organisation of lecture material. The drawings are pedagogical schematics, not reproductions of the original photographs or quantitative experimental graphs. Some explanatory transitions and standard textbook equations are supplied to make the narrative self-contained; they should not be mistaken for verbatim translations of the slides. No exercises or solutions are included.

Contents

Chapter 1

Introduction and Classification of Plasmas

1.1 What is a plasma?

A plasma is an ionized gas containing mobile electrons, ions and, in many practical cases, a large population of neutral atoms or molecules. The charged species respond to electromagnetic fields and generate fields through their own charge and current distributions. Collective behavior, rather than ionization alone, distinguishes plasma physics from ordinary gas kinetics. The original lecture notes emphasize electrical conductivity, optical emission, and the continuous transition between gas and plasma.

1.2 Ionization fraction and plasma regimes

For a singly ionized gas, the ionization fraction is

$$x = \frac{n_i}{n_i + n_g}, \tag{1.1}$$

where n_i is the ion density and n_g the neutral density. In many low-temperature discharges, $x \ll 1$: the plasma is weakly ionized, although its electrons may have energies of several electronvolts. The distinction between *electron temperature* and *gas temperature* is essential.

1.3 Production mechanisms and applications

Plasmas are created by thermal ionization, electric fields in gas discharges, or ionizing radiation. Low-temperature plasmas are particularly important in semiconductor etching, surface activation, deposition, sterilization, lighting and electric propulsion. Direct-current (DC), radio-frequency (RF), and microwave sources are common. Energy supplied to electrons drives excitation, dissociation and ionization; collisions and transport to walls remove particles and energy.

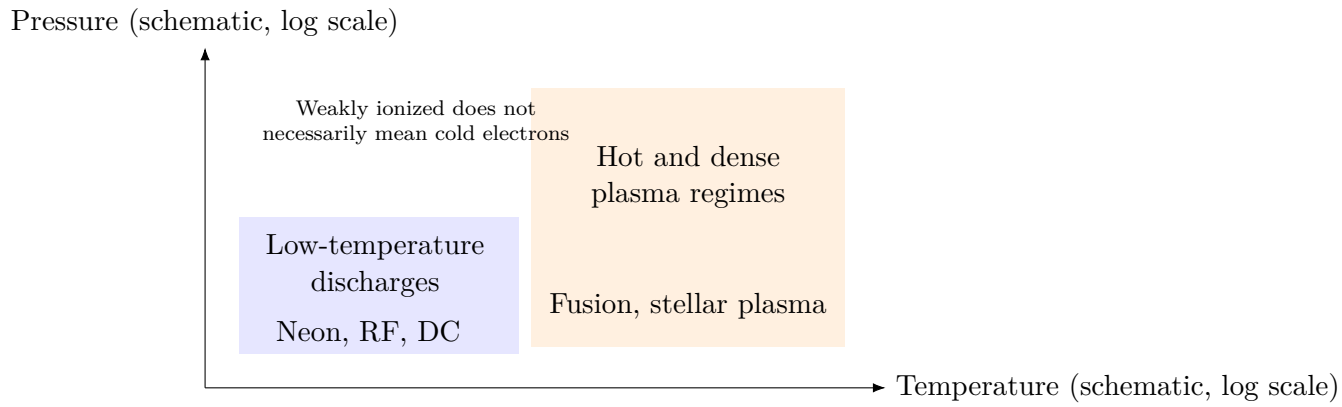


Figure 1.1: Schematic comparison of plasma regimes, redrawn for this script. The regions are illustrative rather than quantitative phase boundaries.

1.4 Typical properties of low-pressure discharges

The source describes low-pressure discharges in the approximate range 0.1–100 Pa, with electron energies $k_B T_e \sim 1$–$10\,\mathrm{eV}$ and substantially colder heavy particles. Typical operating values depend strongly on gas, geometry and power coupling. Electron-neutral collisions, continuous ionization and wall losses must all be included in a physical description. In the quasi-neutral bulk, $n_e \simeq n_i$ for singly charged ions, while this equality generally fails in the sheath.

Chapter 2

Foundations: Fields, Kinetics and Screening

2.1 Self-consistent electromagnetic fields

Plasma particles obey the Lorentz force

$$m_s \frac{d\mathbf{v}}{dt} = q_s(\mathbf{E} + \mathbf{v} \times \mathbf{B}), \tag{2.1}$$

while the fields satisfy Maxwell's equations:

$$\nabla \cdot \mathbf{E} = \rho/\varepsilon_0, \qquad \nabla \cdot \mathbf{B} = 0, \tag{2.2}$$

$$\nabla \times \mathbf{E} = -\partial_t \mathbf{B}, \qquad \nabla \times \mathbf{B} = \mu_0 \mathbf{J} + \mu_0 \varepsilon_0 \partial_t \mathbf{E}. \tag{2.3}$$

Charge conservation follows as $\partial_t \rho + \nabla \cdot \mathbf{J} = 0$. For electrostatic fields $\mathbf{E} = -\nabla\phi$, giving Poisson's equation

$$\nabla^2 \phi = -\frac{\rho}{\varepsilon_0}, \qquad \rho = \sum_s q_s n_s. \tag{2.4}$$

This coupling between particle motion and fields is a defining self-consistency requirement.

2.2 Kinetic distribution functions

For each species s, the distribution $f_s(\mathbf{r}, \mathbf{v}, t)$ describes the phase-space population; its velocity moments yield macroscopic observables:

$$n_s = \int f_s \, d^3v, \qquad n_s \mathbf{u}_s = \int \mathbf{v} f_s \, d^3v. \tag{2.5}$$

The kinetic transport equation is

$$\partial_t f_s + \mathbf{v} \cdot \nabla_{\mathbf{r}} f_s + \frac{q_s}{m_s}(\mathbf{E} + \mathbf{v} \times \mathbf{B}) \cdot \nabla_{\mathbf{v}} f_s = C_s[f], \tag{2.6}$$

where C_s denotes collisions. Setting $C_s = 0$ gives the Vlasov equation. A Maxwellian equilibrium distribution is

$$f_M(\mathbf{v}) = n \left(\frac{m}{2\pi k_B T} \right)^{3/2} \exp\left[-\frac{m|\mathbf{v} - \mathbf{u}|^2}{2k_B T} \right]. \tag{2.7}$$

2.3 Debye shielding and quasi-neutrality

Mobile charges rearrange around a test charge and screen its electric field. In the linear screening approximation,

$$\phi(r) = \frac{Q}{4\pi\varepsilon_0 r}\exp(-r/\lambda_D), \qquad \frac{1}{\lambda_D^2} = \sum_s \frac{n_s q_s^2}{\varepsilon_0 k_B T_s}. \tag{2.8}$$

The second expression assumes suitable thermal species and equilibrium linear response. In many discharge models an electron Debye length $\lambda_{De} = \sqrt{\varepsilon_0 k_B T_e/(n_e e^2)}$ is used as a characteristic scale. Quasi-neutrality is appropriate on spatial scales large compared with the relevant shielding length, except near boundaries and strong gradients.

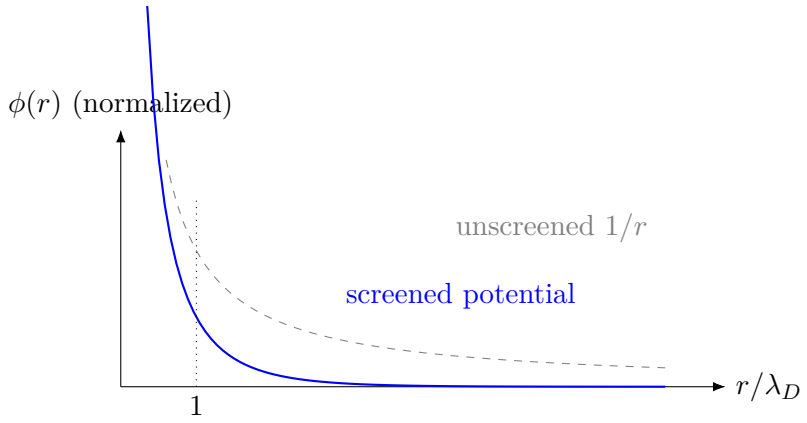


Figure 2.1: Qualitative reduction of the electrostatic potential by Debye screening.

Chapter 3

Collision Dynamics

3.1 Collision processes

Binary collisions transfer momentum and energy and can change internal atomic states. For low-temperature noble-gas discharges the principal processes are electron-neutral elastic scattering, electronic excitation, electron-impact ionization, ion-neutral elastic scattering and resonant charge exchange. In molecular gases, dissociation, attachment and additional reaction channels become important.

3.2 Cross sections and mean free paths

The collision cross section σ describes the effective probability of an interaction. For a stationary uniform background of density n_g, the mean free path and collision frequency are approximately

$$\lambda_{\mathrm{mfp}} = \frac{1}{n_g \sigma}, \qquad \nu = n_g \sigma v. \tag{3.1}$$

When the cross section depends on relative speed, the appropriate rate coefficient is $K = \langle \sigma(v_r) v_r \rangle$, with the average taken over the relative-velocity distribution. Then the reaction rate per unit volume for two species is typically $R = n_a n_b K$.

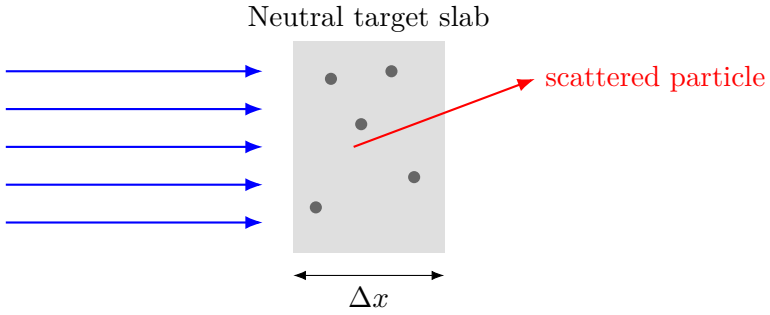


Figure 3.1: Particle transport through a neutral target region, illustrating collisions and attenuation.

3.3 Differential and momentum-transfer cross sections

The differential cross section $d\sigma/d\Omega$ specifies the angular distribution. The total and momentum-transfer cross sections are

$$\sigma_{\mathrm{tot}} = \int \frac{d\sigma}{d\Omega}\, d\Omega, \tag{3.2}$$

$$\sigma_{\mathrm{mt}} = \int (1-\cos\theta)\frac{d\sigma}{d\Omega}\, d\Omega. \tag{3.3}$$

The factor $1-\cos\theta$ reduces the contribution of small-angle scattering to momentum transfer. This distinction matters for transport coefficients and Coulomb scattering.

3.4 Excitation, ionization and charge exchange

Electron-impact ionization requires incident energies above the ionization threshold U_{iz}. Argon has $U_{\mathrm{iz}} \approx 15.76\,\mathrm{eV}$ in the source. The ionization rate depends on the high-energy tail of the electron energy distribution, not simply its mean energy. Resonant charge exchange, such as $\mathrm{Ar}^{+}_{\mathrm{fast}} + \mathrm{Ar}_{\mathrm{slow}} \rightarrow \mathrm{Ar}_{\mathrm{fast}} + \mathrm{Ar}^{+}_{\mathrm{slow}}$, is especially important in weakly ionized gases because it redistributes directed ion motion.

Chapter 4

Plasma Dynamics and Oscillations

4.1 Charged-particle motion

In a uniform magnetic field and with no electric field, a charged particle follows a helix with cyclotron angular frequency and Larmor radius

$$\omega_{cs} = \frac{|q_s|B}{m_s}, \qquad r_{Ls} = \frac{v_\perp}{\omega_{cs}}. \tag{4.1}$$

A static magnetic field does no work: $\mathbf{v} \cdot (\mathbf{v} \times \mathbf{B}) = 0$. In crossed uniform electric and magnetic fields, the guiding center drifts at

$$\mathbf{v}_{E\times B} = \frac{\mathbf{E} \times \mathbf{B}}{B^2}, \tag{4.2}$$

independent of particle mass and charge sign. This principle underlies magnetron discharges and Hall thrusters.

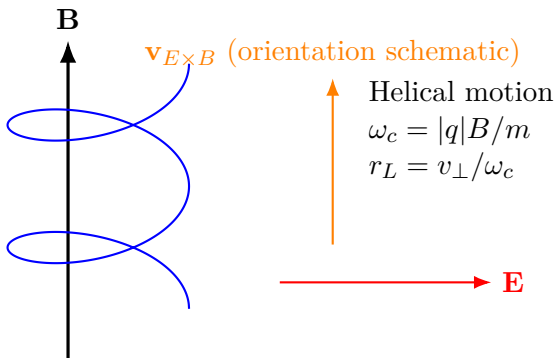


Figure 4.1: Illustrative helical particle motion and crossed-field drift. The elements are schematic and not drawn to a common coordinate scale.

4.2 Plasma frequency

A small displacement of electrons relative to nearly stationary ions produces a restoring electrostatic field. Linearization yields the electron plasma frequency

$$\omega_{pe} = \sqrt{\frac{n_e e^2}{\varepsilon_0 m_e}}, \qquad f_{pe} = \frac{\omega_{pe}}{2\pi}. \tag{4.3}$$

For ions, the corresponding frequency is $\omega_{pi} = \sqrt{n_i Z^2 e^2/(\varepsilon_0 m_i)}$. The thermal speed, plasma frequency and electron Debye length satisfy $\lambda_{De} = v_{Te}/\omega_{pe}$ when $v_{Te} = \sqrt{k_B T_e/m_e}$.

4.3 Collisional response and heating

Under an oscillating field $\mathbf{E}(t)$, electrons accelerate between collisions. A simple momentum balance with effective collision frequency ν_m gives the complex conductivity

$$\sigma(\omega) = \frac{n_e e^2}{m_e(\nu_m - i\omega)}. \tag{4.4}$$

Its dissipative part accounts for collisional (ohmic) electron heating. Plasma oscillations are damped by collisions and may be destabilized by non-equilibrium flows, including two-stream mechanisms.

Chapter 5

Diffusion and Mobility

5.1 Momentum balance in a weakly ionized plasma

For a species with charge q_s, an isothermal pressure gradient and momentum loss to stationary neutrals, the simplified stationary momentum equation reads

$$0 = q_s n_s \mathbf{E} - k_B T_s \nabla n_s - m_s n_s \nu_{sn} \mathbf{u}_s. \tag{5.1}$$

Rearranging gives the drift–diffusion particle flux

$$\mathbf{\Gamma}_s = n_s \mathbf{u}_s = \frac{q_s}{|q_s|} \mu_s n_s \mathbf{E} - D_s \nabla n_s, \tag{5.2}$$

where the positive mobility magnitude and diffusion coefficient are

$$\mu_s = \frac{|q_s|}{m_s \nu_{sn}}, \qquad D_s = \frac{k_B T_s}{m_s \nu_{sn}}. \tag{5.3}$$

Consequently $D_s/\mu_s = k_B T_s/|q_s|$, the Einstein relation under these assumptions.

5.2 Fick's law and continuity

Without an electric field, $\mathbf{\Gamma} = -D\nabla n$. Combining this with particle conservation,

$$\frac{\partial n}{\partial t} + \nabla \cdot \mathbf{\Gamma} = S - L, \tag{5.4}$$

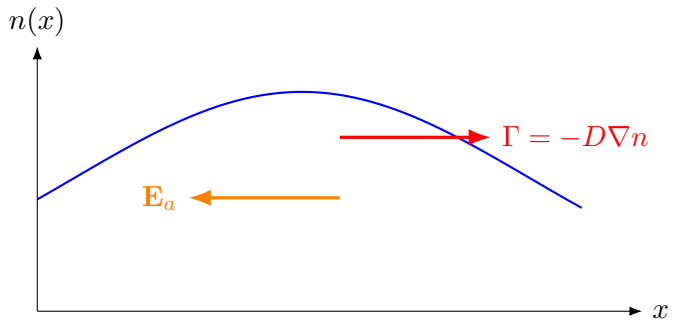
gives the diffusion equation $\partial_t n = D\nabla^2 n + S - L$ for constant D. Here S and L represent local production and loss rates.

5.3 Ambipolar diffusion

Electrons normally diffuse faster than ions. The resulting charge separation creates an ambipolar field that slows electrons and accelerates ions, maintaining approximate quasi-neutrality. For singly charged ions with equal electron and ion particle fluxes,

$$D_a = \frac{\mu_i D_e + \mu_e D_i}{\mu_e + \mu_i}. \tag{5.5}$$

When $\mu_e \gg \mu_i$ and $T_e \gg T_i$, $D_a \simeq \mu_i k_B T_e/e$. These expressions presume a simple collisional drift–diffusion regime; magnetized or strongly nonlocal transport requires modification.



Ambipolar field couples electron and ion transport

Figure 5.1: Density-gradient transport and the ambipolar-field response, schematically.

Chapter 6

The Plasma Boundary and Sheaths

6.1 Why sheaths form

Electrons typically move much faster than ions and initially reach a material surface at a greater rate. An electrically isolated surface therefore charges negatively relative to the plasma. The resulting potential drop repels electrons and accelerates positive ions, forming a non-neutral sheath. The plasma bulk, presheath and sheath have distinct characteristic length scales and physical balances.

6.2 Bohm criterion

In the classical collisionless, cold-ion limit, ions must enter the sheath at or above the Bohm speed

$$u_i \geq c_s, \qquad c_s = \sqrt{\frac{k_B T_e}{m_i}}. \tag{6.1}$$

The presheath accelerates ions toward this threshold. The expression is model-dependent: finite ion temperature, multiple ion species and collisions change the criterion.

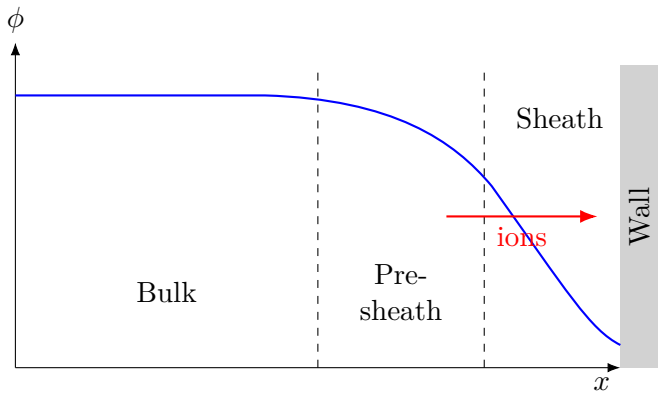


Figure 6.1: Qualitative plasma potential profile from bulk through presheath and sheath to a wall.

6.3 Floating potential and ion bombardment

The floating potential is determined by current balance at an electrically isolated surface. For Maxwellian electrons and idealized ion collection, the electron current decreases exponentially with a negative surface bias, while the ion flux is controlled by presheath and sheath physics. An imposed substrate bias modifies ion impact energy and directionality, making sheaths central to anisotropic etching and sputtering.

6.4 Space-charge-limited current

For an ideal one-dimensional, collisionless planar diode with zero injection speed, the Child–Langmuir law gives

$$j = \frac{4}{9}\varepsilon_0\sqrt{\frac{2|q|}{m}}\frac{V^{3/2}}{d^2}. \tag{6.2}$$

This is a limiting model, not a universal sheath-current formula. It illustrates how space charge constrains current transport across a potential drop.

Chapter 7

Low-Temperature Gas Discharges

7.1 DC breakdown and electron avalanches

In a gas-filled electrode gap, seed electrons are accelerated by an applied electric field. Above sufficient reduced field E/N, electron-impact ionization multiplies the electron population. The first Townsend coefficient α denotes the number of ionizing events per unit path length. In a simple uniform-field model without attachment,

$$n_e(x) = n_e(0)e^{\alpha x}. \tag{7.1}$$

Secondary electron emission at the cathode, often represented by coefficient γ, supports a self-sustaining discharge. The ideal Townsend breakdown condition is

$$\gamma(e^{\alpha d} - 1) = 1. \tag{7.2}$$

7.2 Paschen behavior

The breakdown voltage depends on gas pressure p and electrode separation d. For a fixed gas and ideal geometry, the Paschen curve has a minimum: at very low pressure collisions are too rare; at high pressure the mean energy gained between collisions is too small. Electrode surfaces, impurities and nonuniform fields can strongly affect experimental breakdown.

7.3 Structure of a glow discharge

A DC glow discharge contains a cathode fall, luminous and dark regions, and often a quasi-neutral positive column. The cathode region supports substantial electric fields and secondary-electron production. In the positive column, excitation and ionization maintain the discharge while ambipolar transport supplies losses to walls.

7.4 Capacitively and inductively coupled RF plasmas

In capacitively coupled plasmas (CCPs), RF voltages drive time-dependent electrode sheaths. Displacement current, sheath oscillation and electron heating determine the response. In inductively coupled plasmas (ICPs), an RF coil generates an oscillating magnetic field and induced electric field, transferring energy to electrons without requiring a powered electrode

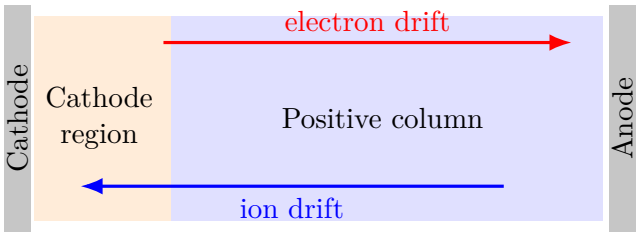


Figure 7.1: Simplified structure of a DC discharge; detailed luminous and dark subregions are omitted.

immersed in the plasma. Microwave discharges use electromagnetic coupling at still higher frequencies. The original notes treat DC, RF and other discharge configurations, including sheath dynamics.

7.5 Particle and power balance

A steady discharge requires volumetric ionization to balance transport and recombination losses. Likewise, absorbed power balances inelastic collisions, elastic heating, radiation and energy carried by particles to walls. These coupled balances explain why discharge density, electron temperature and operating pressure cannot generally be chosen independently.

Chapter 8

Plasma Diagnostics

8.1 Measurement goals and limitations

The source's diagnostics chapter focuses on spectroscopy and Langmuir probes. Measurements may target density, electron energy distributions, excitation and ionization processes, gas composition and spatial gradients. A useful diagnostic must distinguish directly measured signals from plasma parameters inferred through a model.

8.2 Optical emission spectroscopy

Excited atoms, ions and molecules emit photons when they decay to lower energy levels. For a transition $p \to k$ with Einstein coefficient A_{pk}, the local optically thin spectral emissivity integrated over the line is proportional to

$$\epsilon_{pk} \propto n_p A_{pk} h\nu_{pk}. \tag{8.1}$$

The measured line intensity also depends on collection geometry, instrument response, opacity and the spatial distribution of excited states. Excited-state populations depend on electron-impact excitation, radiative decay, cascades, quenching and other collisional processes. Thus line intensity is not in general a direct thermometer. Collisional–radiative modeling is frequently required to infer T_e or n_e.

8.3 Absorption and line profiles

Absorption spectroscopy probes lower-state populations by measuring attenuation of a known light source. Spectral line shapes can carry information about Doppler motion, pressure broadening, Stark effects and instrumental resolution. Doppler broadening may constrain a species' translational temperature only after other broadening mechanisms and nonthermal flows are considered.

8.4 Langmuir probes

A biased electrode immersed in plasma collects electrons and ions. The measured current–voltage characteristic contains an ion-collection region, an electron-retarding region and an

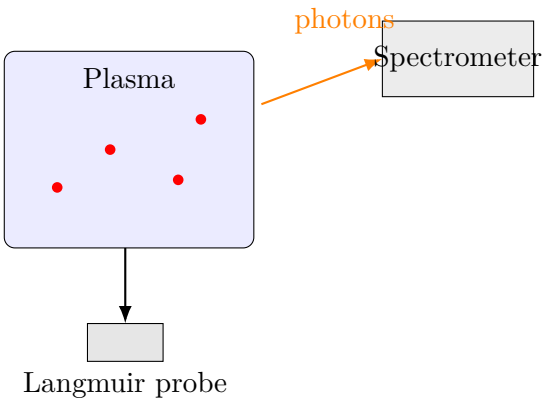


Figure 8.1: Two diagnostics emphasized in the source: passive optical emission spectroscopy and an immersed Langmuir probe.

electron-saturation region. In the electron-retarding region, an ideal Maxwellian model gives approximately

$$I_e(V) \propto \exp\left[\frac{e(V - V_p)}{k_B T_e}\right], \tag{8.2}$$

so the slope of $\ln I_e$ versus probe bias can estimate T_e when the ion current is appropriately subtracted. Density inference depends on collection area and sheath theory. Probe interpretation must account for geometry, contamination, RF fluctuations and deviations from Maxwellian distributions.

8.5 Combining diagnostics with modeling

No single measurement uniquely determines all plasma properties. Spectroscopy provides spatially integrated or resolved radiative information, while probes offer local electrical measurements but perturb the plasma. Comparison with kinetic, fluid or particle-in-cell simulations can test consistency between measured signals and inferred density, temperature and transport parameters.

Source and further reading

- Markus Thoma, *Niedertemperaturplasmaphysik*, supplied lecture slides, 117 pages (primary source for chapter selection and topics).
- M. A. Lieberman and A. J. Lichtenberg, *Principles of Plasma Discharges and Materials Processing* (listed in the source).
- A. Piel, *Plasma Physics* (listed in the source).
- A. von Keudell, *Einführung in die Plasmaphysik*, Ruhr University Bochum lecture notes (listed in the source).